ORGANOMETALLICS

Article

Cite This: *Organometallics* XXXX, XXX, XXX−XXX

Synthesis, Characterization, and Catalytic Properties of Iridium Pincer Complexes Containing NH Linkers

Reuben B. Leveson-Gower,[†] Paul B. Webb,[†] David B. Cordes,[‡] Alexandra M. Z. Slawin,[‡] David M. Smith,[†] Robert P. Tooze,[†] and Jianke Liu*[,†]

[†]Sasol Technology (U.K.) Ltd., Purdie Building, North Haugh, St. Andrews KY16 9ST, U.K.

[‡]School of Chemistry, University of St. Andrews, Purdie Building, North Haugh, St. Andrews KY16 9ST, U.K.

Supporting Information

ABSTRACT: A series of *tert*-butyl-substituted pincer ligands based on 1,3-diaminobenzene and 3-aminophenol scaffolds, ^{tBu4}PXCYP (**1e**, X = Y = NH; **1f**, X = NH; Y = O) and the corresponding iridium hydridochloro complexes (^{tBu4}PXCYP)IrHCl (**2e**, X = Y = NH; **2f**, X = NH; Y = O) were prepared with moderate yields and high purity and were fully characterized by ^{1}H and ^{31}P NMR spectroscopy. Unsymmetrical hybrid pincer ligands ^{R2}PNCOP^{tBu2} (**1g**, R = isopropyl; **1h**, R = cyclohexyl) were prepared conveniently in high yield via a one-pot procedure by judiciously choosing reaction conditions and base; the corresponding iridium hydrido chloro complexes ^{iPr2}PNCOP^{tBu2}IrHCl (**2g**) and ^{Cy2}PNCOP^{tBu2}IrHCl (**2h**) were synthesized by the reaction of $[IrCl(COE)_2]_2$ with ligands. X-ray crystallography reveals that these iridium pincer complexes adopt similar square-pyramidal geometries and exhibit strong intermolecular hydrogen bonding between the NH linker and chloride ions of the adjacent iridium complex in the solid state. ^{1}H NMR chemical shifts of *tert*-butyl based pincer ligated iridium hydrides move downfield when the electronegativity of the linker between the benzene backbone and phosphine moiety increases for **2a**, **2e**, **2f**, and **2b**. Accordingly the corresponding iridium pincer carbonyl complexes (^{tBu4}PXCYP)Ir(CO), **3a**, **3e**, **3f**, and **3b** show a blue shift in the CO stretching frequency. The activities of iridium complexes containing NH linkers were briefly examined for transfer dehydrogenation from cyclooctane to *tert*-butylethylene; (^{iPr2}PNCOP^{tBu2})IrHCl (**2g**) exhibits the highest activity among all tested iridium pincer complexes, including the most studied (^{tBu4}PCP)IrHCl (**2a**) and (^{tBu4}POCOP)IrHCl (**2b**). The enhanced catalytic activity could be related to combined electronic and steric effects of the NH/O hybrid linker and different alkyl groups at phosphorus. This new class of iridium pincer complexes could have great implications in catalytic transformation of polar compounds due to the strong hydrogen-bond-donating ability of the NH linker.

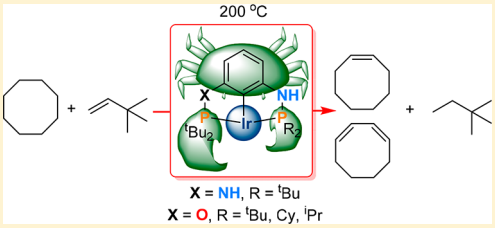

INTRODUCTION

Catalytic alkane dehydrogenation has been extensively studied for a few decades due to its potential importance in the production of linear olefins as versatile chemical intermediates from abundant alkane feedstocks. Pt-based heterogeneous catalysts are widely used in commercial processes to dehydrogenate alkanes to the corresponding alkenes under harsh reaction conditions. Low conversion per pass is essential to maintain high olefin selectivity; thus, alkane dehydrogenation is only operated as an integrated part of the linear alkyl benzene (LAB) production unit to circumvent technical difficulties in product separation. Seminal work by Jensen et al.[1] on homogeneous iridium pincer complex (**2a**, Chart 1) catalyzed alkane dehydrogenation opened up a new avenue for selective functionalization of alkanes. Although other transition metals (Rh, Ru, Os)[2] and phosphine-free pincer ligands such as Phebox[3] have also been explored for alkane dehydrogenation, iridium pincer complexes containing phosphines are the most investigated class due to the great steric and electronic tunability of the pincer ligand framework[4−6] and high thermodynamic driving force for C−H activation by iridium.[7] A significant amount of work has then been dedicated to tuning the steric properties of pincer ligands by altering alkyl groups at the phosphorus atom of Jensen's PCP system.[8] For example,

Chart 1. Iridium Pincer Complexes for Alkane Dehydrogenation

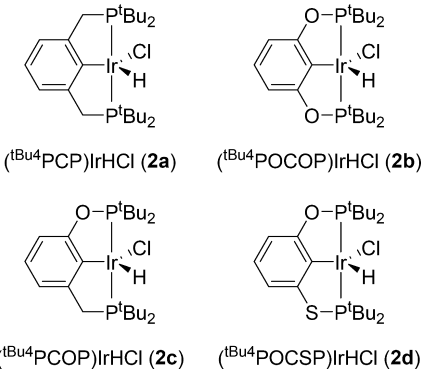

(^{tBu4}PCP)IrHCl (**2a**)
(^{tBu4}POCOP)IrHCl (**2b**)
(^{tBu4}PCOP)IrHCl (**2c**)
(^{tBu4}POCSP)IrHCl (**2d**)

Received: September 19, 2017

DOI: 10.1021/acs.organomet.7b00713
Organometallics XXXX, XXX, XXX−XXX

Goldman et al.[9] systematically varied the steric hindrance of ^{R4}PCPIr complexes by sequential replacement of *tert*-butyl groups with methyl groups, and (^{tBu3Me}PCP)IrH_4 was found more active than other variations. Substituting adamantyl for *tert*-butyl significantly improved the thermal stability of iridium pincer complexes,[10] while the activity for alkane dehydrogenation is comparable for (^{Ad4}PCP)IrH_2 (Ad = adamantyl) and ^{tBu4}PCPIrH_2. Brookhart et al. took a different approach and investigated the effect of the linker between benzene backbone and phosphorus atom of ligands on catalytic alkane dehydrogenation activity.[11] Substitution of CH_2 linkers with oxygen afforded the iridium bis(phosphinite) pincer complexes (^{R}POCOP)Ir, which proved to be highly effective catalysts for transfer dehydrogenation of alkanes. The POCOP-ligated iridium complexes are air stable both in the solid state and in solution and are less inhibited by olefin hydrogen acceptor or product; these characteristics are of paramount importance for bulk chemical production. More interestingly, catalytic activity was improved significantly when only one CH_2 linker was replaced with oxygen; the resulting "hybrid" phosphine−phosphinite pincer iridium complex (^{tBu4}PCOP)Ir (**2c**) is 4 times more active than its bis(phosphine) analogue (^{tBu4}PCP)Ir (**2a**) and 8 times more active than its bis(phosphinite) analogue (^{tBu4}POCOP)Ir (**2b**) in the metathesis of *n*-hexane.[12] Among various permutations of linkers and alkyl substitutents, (^{tBu2}PCOP^{iPr2})Ir was found to be the most active. More recently, Huang et al.[13] synthesized a number of iridium complexes supported by hybrid phosphinothio/phosphinite pincer ligands, among which (^{iPr4}POCSP)Ir was found to be a highly active catalyst for transfer dehydrogenation of *n*-alkanes with high regioselectivity for α-olefin formation while the *tert*-butyl substituted analogue (^{tBu4}POCSP)Ir (**2d**) is much less active most likely due to its steric bulkiness.[14] Iridium pincer complexes containing various linkers reported in the literature are summarized in Chart 1.

Significant advances in synthesis and extensive applications of phosphine-based iridium pincer complexes in catalytic alkane dehydrogenation reactions have been reviewed periodically by Goldman,[15,16] Brookhart,[17] and Huang.[18] Encouraged by promising catalytic activities of iridium complexes achieved by systematically tuning both the linker between the benzene backbone and the phosphine moieties and the alkyl substituents at phosphorus, we turned our attention to investigate the potential influence of NH linkers on the catalytic performance of iridium complexes, which has been much less explored for iridium pincers in the literature. In this work we prepared a series of pincer ligands containing NH linkers (Chart 2) and investigated the effect of the NH moiety on the electronic, steric, and catalytic properties of the corresponding iridium complexes.

Although the synthesis of the 1,3-diaminobenzene-based pincer ligand **1e** and the corresponding square-planar complexes of palladium, nickel, platinum,[19] and cobalt[20] have been reported previously by Kirchner et al., the iridium complex of **1e** has not been reported so far to the best of our knowledge. However, the effect of the linker on the electronic properties of a series of (^{tBu4}PXCXP)Ir (X = O, NH, CH_2, S, etc.) complexes has been investigated computationally.[21] The calculated reaction and activation energies for methane C−H addition are very similar for (^{tBu4}PXCXP)Ir (X = NH, **2e**) and (^{tBu4}POCOP)Ir (**2b**), implying the potential of an iridium pincer complex containing an NH linker in alkane activation. The synthesis and structural characterization of **2e** will allow us

Chart 2. Pincer Ligands Containing NH Linker(s) Synthesized in This Work

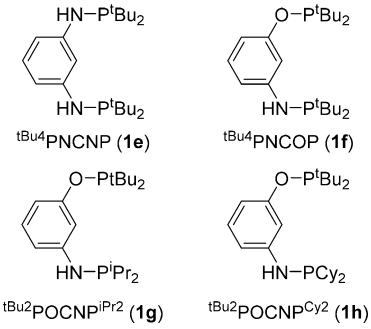

to assess experimentally the effect of O, CH_2, S, and NH linkers on the steric and electronic properties of a complete series of *tert*-butyl-substituted iridium pincer complexes. In comparison to benzene-based pincer ligands with CH_2, O, and S linkers, pincer ligands containing NH linkers could exhibit a very rich chemistry, since NH in close proximity to a metal center will be acidic and can function as a hydrogen bond donor to facilitate polar bond activation. A promising catalytic performance of iridium pincer complexes bearing NH linkers in dehydrogenation of alcohols and hydrogenation of carbonyl compounds can be anticipated. From the perspective of ligand design, the NH moiety also introduces an additional anchor point for further ligand modification to enable precise tuning of the steric crowding about the metal center. Hence, the NH linker will open new avenues for the rational design of new pincer ligands for a wide range of applications.

In this study, we aimed to develop a simple modular procedure to synthesize a series of 3-aminophenol-based unsymmetrical pincer ligands ^{tBu2}POCNP^{R2} (R = ^{t}Bu, **1f**; R = ^{i}Pr, **1g**; R = cyclohexyl (Cy), **1h**) by independently varying the linker, the alkyl substituents at phosphorus, or both. These novel iridium complexes with symmetric and nonsymmetric pincer ligands, **2e−h**, were then prepared and fully characterized by ^{1}H, ^{31}P{^{1}H}, ^{13}C{^{1}H} NMR spectroscopy and X-ray crystallography. The influence of the NH linker on the electronic properties of iridium pincer complexes was probed via the CO stretching frequency of the corresponding iridium pincer carbonyl. Initial catalytic tests were also carried out to compare newly prepared iridium pincer complexes with the widely studied (^{tBu4}PCP)Ir (**2a**) and (^{tBu4}POCOP)Ir (**2b**) for benchmark transfer dehydrogenation of cyclooctane (COA) with *tert*-butylethylene (TBE).

RESULTS AND DISCUSSION

Synthesis of Pincer Ligands. The pincer ligands **1e,f** containing NH linkers are conveniently prepared by diphosphorylation of 1,3-diaminobenzene or 3-aminophenol, respectively, with di-*tert*-butylchlorophosphine (Scheme 1).

The strength of the base was found to be a crucial factor for successful ligand synthesis. Sodium hydride was used as a base for the synthesis of ^{tBu4}POCOP (**1b**) in the literature; a sufficiently stronger base such as *n*-butyllithium is required in this study to deprotonate amino functional groups in 1,3-diaminobenzene and 3-aminophenol because amino groups (pK_a(anline) = 30.7)[22] are much less acidic than the hydroxyl groups of resorcinol (pK_a = 9.15).[23] It is worth highlighting that triethylamine and *n*-butyllithium were added sequentially for the preparation of **1e** in the literature,[19] while *n*-butyllithium

DOI: 10.1021/acs.organomet.7b00713
Organometallics XXXX, XXX, XXX−XXX

Scheme 1. Synthesis of *tert*-Butylphosphorus-Substituted Pincer Ligands 1e,f

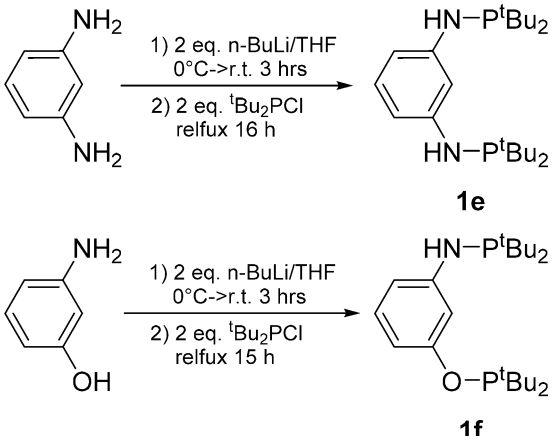

alone is effective in our synthesis. The pincer ligand **1e** was obtained in high yield; its $^{31}P\{^{1}H\}$ NMR spectrum displays a characteristic singlet at 57.8 ppm. The *tert*-butyl-substituted aminophosphine-phosphinite hybrid pincer ligand **1f** was obtained in lower yield and exhibits two singlets at 58.7 and 152.4 ppm, corresponding to the aminophosphine and phosphinite moieties of the NH and O arms, respectively. The isopropyl-substituted analogue of **1f** was prepared previously by Ozerov et al.[24] using a similar procedure and displays singlets at 48.9 and 145.5 ppm in the $^{31}P\{^{1}H\}$ NMR spectrum.

We also extended our synthesis to prepare unsymmetrical PNCOP hybrid pincer ligands **1g,h** through the modular approach shown in Scheme 2.

Scheme 2. One-Pot, Two-Step Synthesis of Unsymmetrical Hybrid Pincer Ligands 1g,h

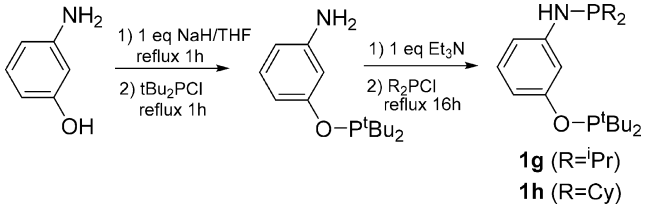

By judiciously choosing reaction conditions and base, **1g,h** were conveniently obtained in high yield and high purity from a one-pot, two-step synthesis. In the first step, the hydroxyl group of 3-aminophenol was selectively deprotonated by 1 equiv of sodium hydride; subsequent addition of 1 equiv of di-*tert*-butylchlorophosphine afforded a monophosphorylated intermediate. In the second step, the intermediate thus obtained was phosphorylated (without isolation and purification) using diisopropylchlorophosphine with triethylamine as a base. Ligand **1g** was obtained in high yield. When dicyclohexylchlorophosphine was used in the second step, the corresponding pincer ligand **1h** was obtained in high yield.

Huang et al. previously synthesized a series of PSCOP pincer ligands with varying alkyl substituents at the S and O arms.[14] However, the monophosphorylated intermediate was separated and purified prior to the introduction of the second dialkylchlorophosphine. The one-pot, two-step synthesis reported here presents obvious advantages due to its simplicity and could be applicable to the synthesis of other pincer ligands with similar structures. The two steps are believed to proceed via different reaction mechanisms due to the different steric bulk of chlorodialkylphosphines and the strength of the base used, as proposed in Scheme 3. Direct deprotonation of the

Scheme 3. Proposed Reaction Mechanism for One-Pot Synthesis of Unsymmetrical Hybrid Ligands

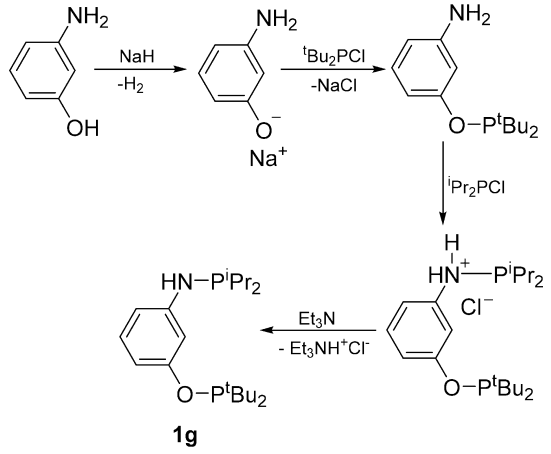

hydroxyl group of 3-aminophenol with a strong base such as sodium hydride in the first step forms the corresponding sodium phenoxide as a strong nucleophile. This subsequently attacks di-*tert*-butylchlorophosphine to afford a monophosphorylated intermediate, while the amino group remains intact due to its low acidity and low nucleophilicity in comparison to the phenoxide anion. In the second step, substitution of diisopropylphosphine at the amino nitrogen atom might proceed via an ammonium salt intermediate, as shown in Scheme 3. It is proposed that the lower steric bulk of the isopropyl groups (in comparison to *tert*-butyl groups) allows for attack by amine as a relatively weaker nucleophile. Conversely, anionic arylamide or phenoxide nucleophiles are required for introduction of di-*tert*-butylphosphine at amino nitrogen and alcohol oxygen atoms, respectively. The acidic ammonium salt intermediate is then deprotonated by a relatively weak base such as triethylamine to afford **1g** as the final product. Such a reaction pathway appears to be limited to less sterically bulky dialkylphosphines, and a slight excess of di-*tert*-butylchlorophosphine introduced in the first step does not affect the second step and can be removed under reduced pressure at the end of the synthesis.

Synthesis of Iridium Complexes. The crude pincer ligands **1e−h** prepared above were used without any further purification, and their reaction with $[IrCl(COE)_2]_2$ in refluxing toluene yields the corresponding iridium pincer hydridochloro complexes **2e,f** with high purity in moderate yields (Scheme 4). The most widely studied iridium pincer complexes, (^{tBu}PCP)-IrHCl (**2a**) and (^{tBu}POCOP)IrHCl (**2b**), were also prepared as reference materials, according to the literature procedure.[11]

The ^{1}H NMR spectra of (^{tBu4}PNCNPIr)HCl (**2e**) and ^{tBu4}PNCOPIrHCl (**2f**) show overlapping doublets or triplets from the *tert*-butyl groups in the narrow range of 1.15−1.3 ppm and triplets from the hydridic IrH moieties at −42.87 (**2e**) and −42.13 ppm (**2f**) with $^{2}J_{PH}$ = 13.0 Hz. The unsymmetrical hybrid pincer iridium complexes (^{iPr2}PNCOP^{tBu2})IrHCl (**2g**) and ^{Cy2}PNCOP^{tBu2}IrHCl (**2h**) also display characteristic IrH triplets at −40.85 and −39.89 ppm, respectively. $^{31}P\{^{1}H\}$ NMR

DOI: 10.1021/acs.organomet.7b00713
Organometallics XXXX, XXX, XXX−XXX

Scheme 4. Syntheses of Pincer-Ligated Iridium Hydrido Chloride Complexes

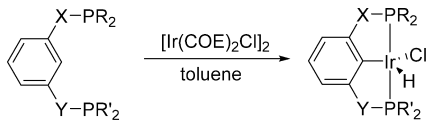

1a-b,1e-h 2a-b,2e-h

	X	Y	R	R'
2a	CH_2	CH_2	tBu	tBu
2b	O	O	tBu	tBu
2e	NH	NH	tBu	tBu
2f	NH	O	tBu	tBu
2g	NH	O	iPr	tBu
2h	NH	O	Cy	tBu

spectra of the hybrid PNCOP iridium pincer complexes **2f–h** present characteristic doublets with $^2J_{PP}$ = 362 Hz from the coupling between the two magnetically inequivalent phosphorus atoms. The iridium pincer hydridochlorides with NH linker(s) synthesized here, **2e–h**, have spectroscopic features similar to those reported previously for **2a–d** containing O and S linkers.[12,14] The ^{1}H NMR chemical shifts of these iridium hydrides are compared in Table 1.

The hydride NMR chemical shifts give some indication of the electronic properties of the metal center and are influenced by the other ligands. For the iridium complexes with symmetrical linkers between the benzene ring and phosphorus atoms, the chemical shift of the iridium hydride resonance moves downfield from −43.48 ppm (**2a**) to −42.87 ppm (**2e**) and −41.4 ppm (**2b**). Ostensibly, this trend indicates decreasing electron density at the iridium metal centers of **2a**, **2e**, and **2b**, which is in good agreement with increasing electronegativity of the linker atom: C (2.55) < N (3.04) < O (3.44). However, the iridium pincer hydrides with mixed linker atoms between the benzene ring and phosphorus donor atoms (^{tBu4}PCOP)IrHCl (**2c**), (^{tBu4}PSCOP)IrHCl (**2d**), and (^{tBu4}PNCOP)IrHCl (**2f**) exhibit hydride resonances in the narrow range of −41.38 to −42.13 ppm, showing no correlation with the electronegativity of different combinations of CH_2, S, NH, and O linkers. Furthermore, ^{1}H NMR chemical shifts of the complexes are apparently affected by the bulkiness of alkyl substituents on the phosphorus atoms. For the series of unsymmetrical PNCOP iridium complexes, a hydride resonance is present at −42.13 ppm for (^{tBu4}PNCOP)IrHCl (**2f**), while it shifts downfield to −40.85 and −39.89 ppm for (^{iPr2}PNCOP^{tBu2})IrHCl (**2g**) and (^{Cy2}PNCOP^{tBu2})IrHCl (**2h**), respectively. Apparently, the hydride chemical shift is not a reliable measure for the estimation of the electronic properties of the metal center in these iridium pincer complexes. One possible explanation could involve spin–orbit coupling (SOC) induced heavy atom effects on the hydride shifts, as revealed by DFT calculations.[25] The SOC effect is particularly significant for iridium hydride complexes and is thought to be predominantly responsible for the unusually high field ^{1}H chemical shifts observed. In contrast, the electronic/steric influence of linkers and alkyl substituents at the phosphorus atom, which are removed from the hydride ligand, become minuscule. Other factors such as π conjugation between the p orbital of linker atoms with lone pairs and the molecular orbitals of the benzene ring also cannot be neglected. The electronegative linker atoms could have two opposite effects: on one hand, they withdraw electron density from phosphorus and reduce the electron-donating abilities of phosphine ligands; on the other hand, they could direct electron flow through π conjugation with the benzene ring and ultimately donate at least part of the electron density originating from the phosphine back to the metal center. The net effect of the linker groups on the electronic properties of the metal center is thus very complex and cannot be solely explained by a single spectral descriptor such as the chemical shifts of iridium hydrides. Nevertheless, iridium pincer hydrido chloro complexes generally serve as catalyst precursors for alkane dehydrogenation, and so it is more preferable to investigate the electronic properties of 14-electron, 3-coordinate iridium pincer intermediates believed to be more relevant for alkane dehydrogenation under the reaction conditions.[17]

CO Stretching Vibration as a Probe of the Structure of Iridium Pincer Complexes. The CO stretching frequency is widely used to determine the small changes in electron density at the metal center of transition-metal carbonyl complexes.[26] Brookhart et al. demonstrated that the shifts of CO stretching frequency (ν_{CO}) of iridium pincer carbonyl complexes are well correlated with the electronic properties of para substituents at the benzene backbone[27] and Lewis acid–base interactions with the γ-alumina support for immobilized iridium catalysts.[28] To probe the electronic properties of catalytically relevant iridium centers, (^{tBu4}PNCNP)Ir(CO) (**3e**) and (^{tBu4}PNCOP)Ir(CO) (**3f**) were prepared in almost quantitative yield using modified literature procedures,[27] as shown in Scheme 5.

Scheme 5. Syntheses of Pincer-Ligated Iridium Monocarbonyl Complexes 3e,f

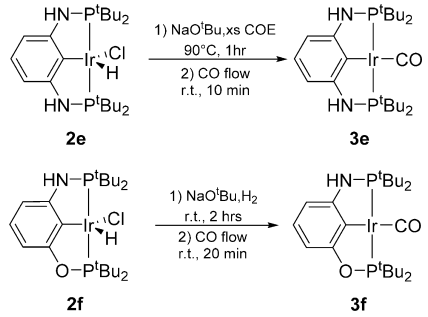

Table 1. ^{1}H NMR Chemical Shifts of Iridium Hydrides Supported by Pincer Ligands with Varying Linkers

	2a	2e	2b	2c	2d	2f	2g	2h
linker (−X−)	CH_2	NH	O	CH_2/O	S/O	NH/O	NH/O	NH/O
δ_H(IrH)/ppm	−43.48	−42.87	−41.40	−41.38	−41.5	−42.13	−40.85	−39.89
$^2J_{PH}$/Hz	12.6	13.0	13.1	13.3, 12.3	14	13.1	13.2	13.1

DOI: 10.1021/acs.organomet.7b00713
Organometallics XXXX, XXX, XXX–XXX

The ν_{CO} stretching frequencies of the resulting carbonyl complexes **3e,f** are compared in Table 2 with those of ^{tBu4}PCP (**3a**) and ^{tBu4}POCOP (**3b**) iridium carbonyls reported previously.

Table 2. CO Stretching Frequencies of Iridium Pincer Carbonyl Complexes

complex	ν_{CO} (cm^{-1})	conditions	ref
^{tBu4}PCPIr(CO) (**3a**)	1913	DCM soln	29
	1917	C_6H_6 soln	9
	1927.7	pentane soln	27
^{tBu4}POCOPIr(CO) (**3b**)	1949	pentane soln	27
	1937	DCM soln	30
^{tBu4}PNCNPIr(CO) (**3e**)	1919.5	DCM soln	this work
^{tBu4}PNCOPIr(CO) (**3f**)	1928.2	DCM soln	this work

As shown in Table 2, ν_{CO} stretching frequencies of the iridium pincer carbonyl complexes vary depending on the solvent in which the infrared spectra were recorded. The IR spectra of **3e,f** were recorded in dichloromethane (DCM) due to their high solubilities in this solvent. IR spectra of **3a**, **3e**, and **3b** in DCM show a blue shift of the ν_{CO} stretching frequencies with increasing electronegativity of the linkers: from 1913 cm^{-1} for **3a** (X = CH_2) to 1919.5 cm^{-1} for **3e** (X = NH) and 1937 cm^{-1} for **3b** (X = O). The blue shift of ν_{CO} is consistent with the decreasing electron-donating properties of iridium pincer fragments in the order **3a** > **3e** > **3b**, as would be expected. The iridium pincer carbonyl with an NH/O hybrid linker (**3f**) displays a CO absorption band at 1928.2 cm^{-1}, which lies between those of **3e** and **3b**, indicating that the effect of the linker on the electronic properties of the metal center might be additive. It is interesting to note that varying the linker between the benzene backbone and phosphorus donor atom is more effective in tuning the electronic properties of metal center than altering alkyl substituents at phosphorus atoms. In this work, ν_{CO} stretching frequencies of (^{tBu4}PXCXP)Ir(CO) can be tuned over a much wider range from 1913 to 1937 cm^{-1}, when the linker X is changed from CH_2 to O and NH. In contrast, ν_{CO} stretching frequencies of (^{R4}PCP)Ir(CO) in hexane solutions vary within a narrow range when the alkyl substituent R is changed from ^{t}Bu (1914 cm^{-1}) to ^{i}Pr (1918 cm^{-1}) and to adamantyl (1916 cm^{-1}).[10] The CO stretching frequency is slightly more sensitive for (^{R4}POCOP)Ir(CO) complexes; a red shift of 7 cm^{-1} from (^{iPr4}POCOP)Ir(CO) (1944 cm^{-1}) to (^{tBu4}POCOP)Ir(CO) (1937 cm^{-1}) was observed in DCM, as ^{t}Bu is more electron donating than ^{i}Pr.[30] Both the literature and current work demonstrate that the electronic properties of a pincer-ligated metal center can be fine-tuned by systematic altering the linker, the substituents at the phosphorus atom, or both. Our attempts to prepare the corresponding carbonyl complexes of **2g,h** following the procedure in Scheme 5 were unsuccessful (see the Supporting Information for details), which prevents us from quantitatively measuring the π-back-donation ability of (^{iPr2}PNOCOP^{tBu2})Ir and (^{Cy2}PNOCOP^{tBu2})-Ir.

Molecular Structures of Iridium Pincer Complexes. After a systematic spectroscopic study of the electronic properties of newly synthesized iridium pincer complexes **2e–h**, we turned our attention to the structural properties of these iridium complexes.[17] Good-quality crystals of iridium complexes **2e–h** were recrystallized from toluene and characterized by X-ray crystallography (Figure 1).

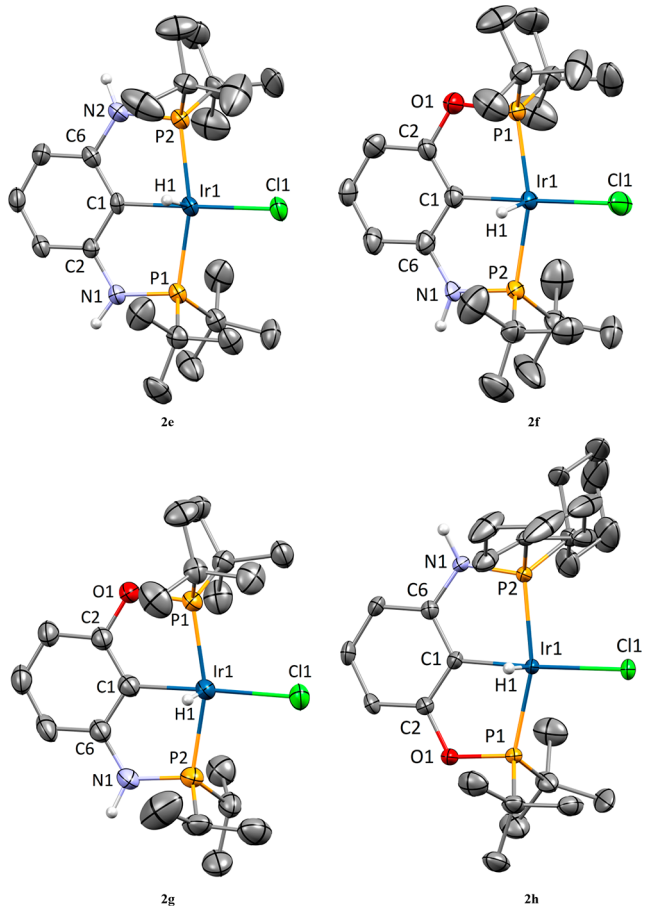

Figure 1. Thermal ellipsoid plots of compounds **2e–h** with thermal ellipsoids at the 50% probability level. Solvent molecules, as well as hydrogen atoms bound to carbon, are omitted for clarity, as is the second independent molecule in **2g**.

As can be seen from Figure 1, all four new iridium pincer complexes synthesized adopt a square-pyramidal geometry with the hydride at the apical site with a vacant position trans to the hydride. Selected bond lengths and bond angles of **2e–h** are compared with those of previously reported iridium pincer complexes **2a–d** in Table 3.

The Ir–C bond lengths are almost identical for all iridium pincer complexes and fall in the range of 2.011–2.019 Å. A closer inspection reveals the structural difference between the newly synthesized **2e,f** and the well-studied **2a,b**. The structures of **2a,b** are almost perfectly square pyramidal; the C1–Ir–Cl1 angles of **2a** (179.7°) and **2b** (179.11°) are very close to linearity.[32] New iridium pincer complexes prepared in this work exhibit large distortion angles C1–Ir–Cl1 of 177.22, 178.8, 173.91. and 170.88° for **2e–h**, respectively. Such large distortion from a perfect square-pyramidal geometry could be attributed to electronic effects of the NH and/or O linkers (**2e,f**), steric effects of alkyl substituents at the NH linker (**2f–h**), or both. However, extensive hydrogen-bonding interactions between the chloride and amide moieties ($r_{N-H\cdots Cl}$ = 3.266–3.360 Å) were observed for all iridium pincer hydrido chloro complexes containing the NH linker, **2e–h**, in the solid state, and this could play a dominant role in the structural distortion observed. The influence of hydrogen bonding on structural distortion is most profound for **2e**. Unexpectedly different Ir–P bond lengths, Ir–P1 = 2.2935(13) Å and Ir–P2 = 2.3186(13) Å, were observed for this highly symmetrical complex. This can

DOI: 10.1021/acs.organomet.7b00713
Organometallics XXXX, XXX, XXX–XXX

Table 3. Selected Bond Lengths and Bond Angles for Complexes 2e−h[31]

complex	linker	Ir−C1 (Å)[a]	Ir−P1 (Å)[b]	Ir−P2 (Å)[b]	Ir−Cl1 (Å)	P1−Ir−P2 (deg)[c]	C1−Ir−Cl1 (deg)	ref
2b	O	2.010	2.297	2.293	2.404(1)	160.06	179.11(14)	14
2e	NH	2.019(4)	2.2937(13)	2.3186(13)	2.4245(13)	163.44(5)	177.22(13)	this work
2a	CH_2	2.014	2.305	2.305	2.425	164.27	179.7(2)	10
2f	NH/O	2.011(8)	2.278(2)	2.310(2)	2.401(3)	161.88(8)	178.8(3)	this work
2c	CH_2/O	2.016	2.3194	2.2685	2.4012(10)	163.55	177.71(9)	12
2d	S/O	2.019	2.2986	2.298	2.4149(8)	168.32	172.97(9)	14
2g	NH/O	2.011(5)	2.2797(12)	2.2904(12)	2.4199(12)	162.14(4)	173.91(14)	this work
2h	NH/O	2.013(3)	2.809(9)	2.2912(10)	2.4127(9)	162.20(3)	170.88(11)	this work

[a]Distance between Ir and C1. [b]The bond lengths Ir−P1 and Ir−P2. [c]Defined as P1^IrP2.

be attributed to the fact that intermolecular hydrogen bonding to the adjacent chloride ion only occurs at one amide moiety (NH−P2) and not the other (NH−P1). The Cl···H−N hydrogen bonding will reduce the electron density of the nearest phosphorus atom P2, and consequently Ir−P2 is elongated with respect to Ir−P1 in **2e**. Closer inspection of the solid-state structure of **2e** shows that intermolecular hydrogen bonding also increases the P2−Ir−C1 bond angle with respect to the P1−Ir−C1 angle.

Despite the distorted-square-pyramidal structures owing to intermolecular hydrogen bonding between chloride and NH moieties, all four iridium pincer complexes containing one or more NH linkers prepared in this work show a pronounced planar structure: i.e., the arene backbone of the pincer ligand is essentially coplanar with the two adjacent five-membered Ir−P−X−C−C chelate rings. The coplanar structure of these iridium pincer complexes could be essential for efficient π conjugation between a lone pair of the NH/O linker and the benzene backbone of the pincer ligand. The resulting stable and rigid structure could confer increased thermal stability which is highly desirable for dehydrogenation reactions.

The steric hindrance of transition-metal complexes is often quantified by the P1−Ir−P2 bite angle, which is invariably altered when different linkers are placed between the benzene backbone and the phosphine moiety. As seen in Table 3 for the series of *tert*-butyl-substituted phosphine-based iridium pincer complexes, the P1−Ir−P2 bite angle of (^{tBu4}PXCXP)IrHCl increases with increasing covalent radii of the linker atoms:[33] 160.06° for **2b** (X = O), 163.44° for **2e** (X = NH), and 164.27° for **2a** (X = CH_2). A similar trend was also observed for unsymmetrical iridium pincer complexes, (^{tBu4}PXCOP)IrHCl, which exhibit increasing P1−Ir−P2 bite angles as the covalent radii of the other linker increases: 161.88° for **2f** (X = NH), 163.55° for **2c** (X = CH_2), and 168.32° for **2d** (X = S). Apparently the steric properties of the iridium pincer complex can be effectively modulated by systematic altering of the linkers and by their combinations. The structural parameters determined above for iridium catalyst precursors in the solid state may not be reflected in the real catalyst under the reaction conditions. However, the structural dependence of iridium pincer complexes on steric/electronic properties of the linkers should follow a trend similar to that observed in the solid state and provide a basis for further study of the structure−activity relationship. Furthermore, the tendency of the NH moiety to function as a strong hydrogen bond donor suggests that the newly prepared iridium pincer complexes might potentially find broad applications especially in catalytic activation and transformation of polar covalent bonds, where effective metal−ligand cooperation would be expected.

Catalytic Activity for Alkane Transfer Dehydrogenation. Catalytic activities of **2e−h** were evaluated for the benchmark transfer dehydrogenation reaction of COA with TBE as a hydrogen acceptor. The catalytic reactions were carried out using a Fischer−Porter bottle with a total volume of ∼20 mL instead of the sealed small-volume glass reactor (∼4 mL) used in the literature;[11] **2e−h** were activated in situ by addition of NaO^{t}Bu under reaction conditions otherwise similar to those employed in the literature.[27] Each catalyst was tested in triplicate, and the catalytic results of **2e−h** are compared with those of the reference catalysts **2a**,**b** in Table 4.

Table 4. Catalytic Test Data for the Benchmark Transfer Dehydrogenation Reaction Using COA and TBE[a]

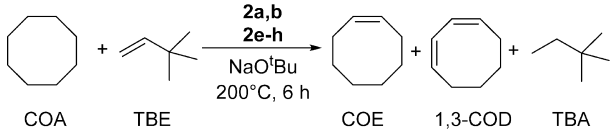

precatalyst	TON (6 h)[b]	COE/(COE + 1,3-COD) (%)[b]
2a	1530	71.6
2b	898	83.4
2e	596	85.9
2f	731	84.2
2g	1627	68.7
2h	1117	72.7

[a]Reaction conditions: [Ir] = 1.1 mM, [COA] = [TBE] = 3.37 M, ∼10 equiv of NaO^{t}Bu, 200 °C, 6 h. [b]Average of three or more runs.

All iridium complexes display considerable activities for COA/TBE transfer dehydrogenation. In addition to cyclooctene (COE) as the expected product from transfer dehydrogenation of COA, substantial amounts of 1,3-cyclooctadiene (1,3-COD) were also produced from consecutive dehydrogenation of COA.[11] As seen from Table 4, the COE content in total products decreases with increasing catalyst activity in the order **2e** < **2f** < **2b** < **2h** < **2a** < **2g**, since more COE underwent further dehydrogenation to 1,3-COD over a more active catalyst. Surprisingly, (^{tBu}PCP)Ir (**2a**) was found to be more active than (^{tBu}POCOP)Ir (**2b**) under the reaction conditions employed in this study. This is completely opposite to what has been reported in the literature: **2a** is at least 8 times less active than **2b** under identical conditions,[11] and the catalytic activity of **2a** is significantly inhibited when the ratio TBE:Ir is >300.[8] The surprisingly high activity of **2a** for the COA/TBE reaction in this study could be attributed to the different experimental setup. The Fischer−Porter bottle reactor used in this study has a large headspace; the ratio between liquid phase and headspace volume is approximately 1:9 under

DOI: 10.1021/acs.organomet.7b00713
Organometallics XXXX, XXX, XXX−XXX

ambient conditions while the ratio was approximately 1:1 for the sealed glass reactor mostly used in the literature.[11,12] It is therefore plausible to postulate that the concentration of TBE in this study would be much lower than that in the literature due to vapor−liquid equilibria; thus, **2a** is much less inhibited by olefins and displays activity comparable to that of **2b**. The catalytic effectiveness of iridium pincer catalysts can be dramatically affected by reaction conditions in addition to many other factors thoroughly reviewed in the literature, such as electronic/steric properties of catalytically active species,[17] the reaction mechanism,[34] and the combination of alkane substrate and hydrogen acceptor.[1] The discrepancy in the relative catalytic transfer dehydrogenations of **2a** and **2b** clearly highlights challenges in a fair and accurate comparison of catalyst performance.

Structural characterization and preliminary catalytic test results in Tables 2−4 do not reveal a clear trend between catalytic performance of iridium pincer complexes with electronic/steric properties of varying linkers or alkyl substituents at phosphorus. However, the results of **2b**,**e**,**f**, *tert*-butyl-substituted pincer iridium complexes with varying linkers, reveal a weak correlation between catalytic activity and the electronic/steric properties described by their C−O stretching frequencies and P−Ir−P bite angles. Their COA/TBE transfer dehydrogenation activities, **2e** (TON = 596), **2f** (TON = 731), and **2b** (TON = 898), increase with decreasing P−Ir−P bite angle (**2e**, 163.44°; **2f**, 161.88°; **2b**, 160.06°) and with increasing electron deficiencies of the iridium center (ν_{CO} 1919.5 cm^{-1} (**3e**), 1928.2 cm^{-1} (**3f**), 1937 cm^{-1} (**3b**)). Thus, a smaller bite angle and more electron deficient metal center seem to favor the COA/TBE reaction for this series of iridium complexes. However, such a trend does not hold for (^{tBu4}PCP)IrHCl (**2a**), which has the largest bite angle and the most electron rich metal center but exhibits the highest activity. We speculate that lone pairs of O and NH linkers could considerably affect the electronic properties of the metal center probably via effective overlapping of the p orbital of the linker atoms with the ring current of benzene backbone, while the overlapping of orbitals is insignificant for (^{tBu4}PCP)IrHCl (**2a**).

For unsymmetrical (^{R2}PNCOP^{tBu2})IrHCl complexes (R= ^{t}Bu (**2f**), ^{i}Pr (**2g**), Cy (**2h**)), the steric properties of alkyl substituents apparently play a dominant role in catalytic activity. The COA/TBE reaction activity increases in the order **2f** (TON = 731) < **2h** (TON = 1117) < **2g** (TON = 1627), with the steric hindrance of alkyl substituents at the NH arm decreasing from ^{t}Bu to Cy to ^{i}Pr. Interestingly, the P−Ir−P bite angles of **2f**−**h** determined by X-ray crystallography are very similar: **2f**, 161.88°; **2g**, 162.14°; **2h**, 162.20°. The catalyst testing protocol used in this study determined the catalytic activity at a single time point and does not take potential catalyst deactivation into consideration, thus presenting an obvious disadvantage for accurate comparison of catalyst performance. Although no catalyst decomposition was noted visually for any of the iridium catalysts during the course of the reaction, a more thorough and reliable catalyst testing is required to establish structure−activity relationships.

In summary, newly synthesized iridium pincer complexes containing NH linkers **2e**−**h** display moderate to high activities for the benchmark COA/TBE transfer dehydrogenation reaction; the highly unsymmetrical hybrid pincer complex (^{iPr2}PNCOP^{tBu2})IrHCl (**2g**) was found to be the most active among the iridium pincer complexes tested. It is difficult to establish a clear correlation between the catalytic performance of iridium pincer complexes and the electronic/steric effects of pincer ligands for several reasons. It is predominantly because the electronic effects cannot be completely separated from the steric effects even with rationally designed and systematically tuned ligand scaffolds. For instance, substitution of the methylene linker for more electronegative O or NH linkers increases the electron deficiency of the iridium metal center but also results in considerable changes in the bond length to neighboring atoms. Second, the catalytic activities were determined at a single time point and may not reflect the intrinsic activities of the catalyst, as potential catalyst deactivation was largely neglected. Nevertheless, iridium pincer complexes with an NH linker prepared in this study exhibit activity comparable to or higher than those of their PCP and POCOP analogues for the COA/TBE benchmark reaction. The NH linker could play a greater role via metal−ligand cooperation, a concept well demonstrated in other catalyst systems with similar ligand scaffolds.[35,36] The potential applications of these novel iridium pincer complexes in other transformations such as linear alkane dehydrogenation, alcohol dehydrogenation, and CO_2 hydrogenation are currently under investigation.

CONCLUSIONS

A simple modular synthetic route has been developed to prepare unsymmetrical hybrid pincer ligands ^{iPr2}PNCOP^{tBu2} (**1g**) and ^{Cy2}PNCOP^{tBu2} (**1h**) in a one-pot process without isolation and purification of the monosubstituted intermediate. The series of iridium pincer complexes (^{tBu4}PNCNP)IrHCl (**2e**), (^{tBu4}PNCOP)IrHCl (**2f**), (^{iPr2}PNCOP^{tBu2})IrHCl (**2g**), and (^{Cy2}PNCOP^{tBu2})IrHCl (**2h**) have been synthesized and fully characterized by ^{31}P, ^{1}H, and ^{13}C NMR spectroscopy and elemental analysis. Single-crystal X-ray crystallography studies show that all iridium pincer complexes synthesized adopt a slightly distorted square pyramidal geometry and exhibit extensive hydrogen bonding between the NH functionality with chloride ions of the adjacent iridium complex in the solid state. The catalytic activities of iridium pincer complexes were evaluated for the benchmark COA/TBE transfer dehydrogenation and compared with those of ^{tBu}PCPIrHCl (**2a**) and ^{tBu}PCPIrHCl (**2b**) reference catalysts. Iridium complexes with NH linkers **2e**−**h** exhibit moderate to high activities for COA/TBE transfer dehydrogenation. (^{iPr2}PNCOP^{tBu2})IrHCl (**2g**), an iridium complex supported by unsymmetrical hybrid pincer ligands with an NH linker, afforded the highest activity among all iridium pincer complexes tested.

EXPERIMENTAL SECTION

General Considerations. All manipulations were carried out under a dry argon atmosphere, using an argon-filled glovebox or using standard Schlenk and cannula techniques. DCM, THF, pentane, and toluene were collected from a Braun solvent purification system and deoxygenated by sparging with argon prior to use. C_6D_6 and CD_2Cl_2 were dried over P_2O_5 and vacuum-transferred prior to use. Resorcinol, 3-aminophenol, *m*-phenylenediamine, ClP^{t}Bu$_2$, ClP^{i}Pr$_2$, sodium hydride, sodium *tert*-butoxide, *n*-butyllithium, P_2O_5, and [IrCl(COE)$_2$]$_2$ were purchased from Sigma-Aldrich and used without further purification. Cyclooctane and 3,3-dimethyl-1-butene were purchased from Sigma-Aldrich and degassed prior to use (the water contents were determined to be 20 and 41 ppm, respectively, by Karl Fischer titration). 1,3-Bis[(di-*tert*-butylphosphino)methyl]benzene (**1a**) was purchased from STREM. NMR spectra were acquired on Bruker AVIII 500 (500 MHz), Bruker AVIII HD-500 (500 MHz), and Bruker AV 400 (400 MHz) spectrometers. Chemical shifts are

DOI: 10.1021/acs.organomet.7b00713
Organometallics XXXX, XXX, XXX−XXX

referenced to residual protio impurities in the deuterated solvent (^{1}H) or the ^{13}C shift of the solvent (^{13}C). Phosphorus chemical shifts are reported without reference. Mass spectra were obtained using a Bruker electrospray ionization (ESI) micrOTOF-Q II mass spectrometer. Elemental analysis was performed using a Thermo Scientific (Carlo Erba) Flash 200 elemental analyzer. IR spectra were recorded on a Nicolet Nexus FT-IR spectrometer.

Synthesis of Pincer Ligands. The ligand ^{tBu4}POCOP(**1b**) was synthesized following literature procedures.[11]

*^{tBu4}PNCNP (**1e**).*[24] A solution of *n*-butyllithium (5.25 mL, 1.1 M in hexane, 5.78 mmol) was slowly added via syringe to a solution of *m*-phenylenediamine (272 mg, 2.5 mmol) in THF (20 mL) cooled to 0 °C. A yellow precipitate was formed; the mixture was stirred for 30 min at 0 °C and then for 3 h at room temperature. The solution was then cooled to 0 °C, and Cl^{t}Bu$_2$ (1.05 mL, 1.00 g, 5.5 mmol) was added dropwise. The solution was warmed to room temperature and then refluxed for 16 h. After evaporation of the solvent under vacuum, the residue was extracted with pentane (3 × 20 mL) and the extract cannula-filtered. The pentane was removed in vacuo to afford **1e** (626 mg, 63% yield).

^{1}H NMR (CD_2Cl_2, 499.93 MHz): δ 6.91 (1H, t, $^3J_{PH}$ = 8.0, Ar-*H*), 6.75 (1H, m, Ar-*H*), 6.38 (2H, dm, $^3J_{PH}$ = 8.0, Ar-*H*), 3.99 (2H, d, $^2J_{PH}$ = 10.9, N*H*), 1.15 (36H, d, $^3J_{PH}$ = 11.8, PC(C*H*$_3$)$_3$). ^{31}P{^{1}H} NMR (CD_2Cl_2, 125.76 MHz): δ 57.8 (s). ^{13}C{^{1}H} NMR (CD_2Cl_2,202.38 MHz): δ 151.0 (C_q, d, $^2J_{PC}$ = 17, *C*(1) and *C*(3)), 129.9 (CH, s, *C*(5)), 107.0 (CH, d, $^3J_{PC}$ = 11.6, *C*(4) and *C*(6)), 103.8 (CH, t, $^3J_{PC}$ = 12.5, *C*(2)), 34.6 (C_q, d, $^1J_{PC}$ = 20.0, *C*(CH$_3$)$_3$), 28.4 (CH$_3$, d, $^2J_{PC}$ = 15.3, C(*C*H$_3$)$_3$).

*^{tBu4}PNCOP (**1f**).* *n*-Butyllithium (5.5 mL, 1.1 M in hexanes, 6.05 mmol) was added dropwise to a solution of 3-aminophenol (273 mg, 2.5 mol) in THF (20 mL) at 0 °C followed by 1 h of stirring. The solution was warmed to room temparture and stirred for a further 3 h, whereupon a copious off-white precipitate had formed. ^{t}Bu$_2$PCl (1.05 mL, 5.5 mmol) was added dropwise to the resulting suspension at 0 °C. The reaction was warmed to room temperature, a condenser was fitted, and the reaction mixture was brought to reflux for 15 h. The volatile components were removed in vacuo, the resulting solid residue was extracted with pentane (2 × 20 mL), and the extract was cannula-filtered. The pentane was removed in vacuo to afford **1f** as a brown solid (452 mg, 45%), which displayed approximately 50% purity by ^{31}P NMR and was used without further purification.

^{1}H NMR (CD_2Cl_2, 500.13 MHz, 300 K): δ 6.98 (apparent t, |2 × $^3J_{HH}$| = 8.1 Hz, 1H, Ar-*H*), 6.83 (m, 1H, Ar-*H*), 6.58 (m, 1H, Ar-*H*), 6.50 (m, 1H, Ar-*H*), 4.03 (d, $^2J_{PH}$ = 10.6 Hz, 1H, N*H*), 1.15 (d, $^3J_{PH}$ = 11.7 Hz, 18H, P-C(C*H*$_3$)$_3$), 1.12 (d, $^3J_{PH}$ = 11.8 Hz, 18H, P-C(C*H*$_3$)$_3$). ^{31}P{^{1}H} NMR (CD_2Cl_2, 202.46 MHz, 300 K): δ 152.4 (s), 58.7 (s). ^{13}C{^{1}H} NMR (CD_2Cl_2, 125.76 MHz, 300 K): δ 161.2 (d, $^2J_{PC}$ = 9.3 Hz, C_{Ar}), 151.3 (d, $^2J_{PC}$ = 17.6 Hz, C_{Ar}), 129.8 (s, C_{Ar}), 109.6 (d, $^3J_{PC}$ = 11.7 Hz, C_{Ar}), 108.5 (d, $^3J_{PC}$ = 10.8 Hz, C_{Ar}), 106.3 (apparent t, |2 × $^3J_{PC}$| = 11.6 Hz, C_{Ar}), 35.8 (d, $^1J_{PC}$ = 25.7 Hz, C_q), 34.4 (apparent t, |2 × $^1J_{PC}$| = 20.2 Hz, C_q), 28.5 (d, $^2J_{PC}$ = 15.0 Hz, CH$_3$), 28.3 (d, $^2J_{PC}$ = 15.2 Hz, CH$_3$), 27.5 (d, $^2J_{PC}$ = 15.4 Hz, CH$_3$).

*General Procedure for Synthesis of Ligands **1g,h**.* In an argon-filled glovebox, 3-aminophenol and sodium hydride (1.1 equiv) were weighed into a Schlenk flask inside a glovebox. THF (20 mL) was added (*caution*! hydrogen evolution), and the resulting suspension was refluxed for 1 h and then cooled to room temperature. Di-*tert*-butylchlorophosphine (1.1 equiv) was added dropwise, and the reaction mixture was refluxed for 1−1.5 h and then cooled to room temperature. After completion of the reaction (indicated by ^{31}P NMR spectroscopy), triethylamine (2 equiv) and then either diisopropylchlorophosphine or dicyclohexylchlorophosphine (1.1 equiv) were added slowly at room temperature. The reaction mixture was refluxed overnight. The volatiles were removed in vacuo, the residue was extracted with pentane, and the extract was cannula-filtered. The pentane was removed in vacuo to obtain the ligands **1g,h**.

*^{iPr2}PNCOP^{tBu2} (**1g**).* From 3-aminophenol (763 mg, 7 mmol), sodium hydride (194 mg, 8 mmol), di-*tert*-butylchlorophosphine (1.7 mL, 8 mmol), triethylamine (2.1 mL, 15 mmol), and diisopropylchlorophosphine (1.3 mL, 8 mmol) **1g** was obtained as a colorless oil (2.98 g) in quantitative yield. The purity was determined to be >90% by ^{31}P NMR, and the ligand was used without further purification.

^{1}H NMR (CD_2Cl_2, 500.13 MHz, 300 K): δ 6.97 (apparent t, |2 × $^3J_{HH}$| = 8.1 Hz, 1H, Ar-*H*), 6.80 (m, 1H, Ar-*H*), 6.54 (m, 1H, Ar-*H*), 6.50 (m, 1H, Ar-*H*), 3.78 (d, $^2J_{PH}$ = 10.2 Hz, 1H, N*H*), 1.74 (m, 2H, P-C*H*(CH$_3$)$_2$), 1.15 (d, $^3J_{PH}$ = 11.7 Hz, 18H, P-C(C*H*$_3$)$_3$), 1.08−1.02 (m, 12H, P-CH(C*H*$_3$)$_2$). ^{31}P{^{1}H} NMR (CD_2Cl_2, 202.46 MHz, 300 K): δ 152.5 (s), 48.4 (s). ^{13}C{^{1}H} NMR (CD_2Cl_2, 125.71 MHz, 300 K): δ 161.2 (d, $^2J_{PC}$ = 9.4 Hz, C_{Ar}), 150.6 (d, $^2J_{PC}$ = 16.4 Hz, C_{Ar}), 129.8 (s, C_{Ar}), 109.4 (d, $^3J_{PC}$ = 11.7 Hz, C_{Ar}), 108.6 (d, $^3J_{PC}$ = 10.6 Hz, C_{Ar}), 106.2 (apparent t, |2 × $^3J_{PC}$| = 11.5 Hz, C_{Ar}), 35.8 (d, $^1J_{PC}$ = 26.2 Hz, C_q), 28.0 (d, $^2J_{PC}$ = 17.0 Hz, CH$_3$), 27.5 (d, $^2J_{Pc}$ = 15.9 Hz, CH$_3$), 27.1 (d, $^2J_{PC}$ = 12.0 Hz, CH$_3$), 19.0 (d, $^1J_{PC}$ = 19.9 Hz, CH), 17.2 (d, $^1J_{PC}$ = 7.8 Hz, CH).

*^{Cy2}PNCOP^{tBu2} (**1h**).* From 3-aminophenol (546 g, 5 mmol), sodium hydride (142 mg, 5.5 mmol), di-*tert*-butylchlorophosphine (1.1 mL, 5.5 mmol), triethylamine (1.4 mL, 10 mmol), and dicyclohexylchlorophosphine (1.2 mL, 5.5 mmol) **1h** was obtained as a white solid (2.03 g, 90%). The purity was determined to be ∼95% by ^{31}P NMR, and the ligand was used without further purification.

^{1}H NMR (C_6D_6, 499.93 MHz, 300 K): δ 7.23 (m, 1H, Ar-*H*), 7.09 (apparent t, |2 × $^3J_{HH}$| = 8.2 Hz, Ar-*H*), 6.88 (m, 1H, Ar-*H*), 6.73 (m, 1H, Ar-*H*), 3.45 (d, $^2J_{PH}$ = 10.7 Hz, 1H, N*H*), 1.73−1.51 (m, 12H, Cy*H*), 1.40−1.32 (m, 2H, Cy*H*), 1.17 (d, $^3J_{PH}$ = 11.6 Hz, 18H, P-C(C*H*$_3$)$_3$), 1.15−1.01 (m, 8H, Cy*H*). ^{31}P{^{1}H} NMR (C_6D_6, 202.38 MHz, 300 K): δ 150.3 (s), 41.0 (s). ^{13}C{^{1}H} NMR (C_6D_6, 125.76 MHz, 300 K): δ 161.4 (d, $^2J_{PC}$ = 9.7 Hz, C_{Ar}), 151.2 (d, $^2J_{PC}$ = 17.0 Hz, C_{Ar}), 130.1 (s, C_{Ar}), 109.8 (d, $^3J_{PC}$ = 12.5 Hz, C_{Ar}), 108.8 (d, $^3J_{PC}$ = 11.7 Hz, C_{Ar}), 106.4 (apparent t, |2 × $^3J_{PC}$| = 11.9 Hz, C_{Ar}), 36.7 (d, $^1J_{PC}$ = 13.1 Hz, CH), 35.7 (d, $^1J_{PC}$ = 26.3 Hz, C_q), 29.4 (d, $^2J_{PC}$ = 18.7 Hz, CH$_2$), 27.6 (d, $^2J_{PC}$ = 15.7 Hz, CH$_3$), 27.5−27.1 (m, CH$_2$), 26.7 (s, CH$_2$).

Synthesis of Iridium Complexes. ^{tBu}PCPIrHCl (**2a**) and ^{tBu}POCOPIrHCl (**2b**) were prepared by following the literature procedure.[11]

*General Procedure for Synthesis of Iridium Complexes **2e−h**.* [IrCl(COE)$_2$]$_2$ and the ligands **1e−h** (∼2.2 equiv) were dissolved in toluene (15 mL) in a Schlenk flask, a condenser was fitted, and the reaction mixture was refluxed overnight (or 4 h for **2h**) and then cooled to room temperature. The toluene was removed in vacuo, and the solid residue was washed with pentane and dried in vacuo to obtain **2e−h**.

*^{tBu4}PNCNPIrHCl (**2e**).* From **1e** (325 mg, 0.83 mmol) and [IrCl(COE)$_2$]$_2$ (347 mg, 0.4 mmol) **2e** was obtained as a brick red solid (215 mg, 45% yield). The solid residue was washed with pentane and then extracted into DCM. The DCM extract was taken to dryness to afford the final product.

Anal. Calcd for $C_{22}H_{42}ClIrN_2P_2$: C, 42.33; H, 6.78; N, 4.49. Found: C, 42.18; H, 6.91; N, 4.34. HRMS: calcd for $C_{22}H_{43}ClIrN_2P_2$ [M + H$^+$], 625.2206; found, *m*/*z* 625.2597. ^{1}H NMR (C_6D_6, 500.13 MHz, 300 K): δ 6.92 (t, $^3J_{HH}$ = 7.7 Hz, 1H, Ar-*H*), 6.24 (d, $^3J_{HH}$ = 7.7 Hz, 2H, Ar-*H*), 4.05 (br s, 2H, N*H*), 1.24 (apparent t, |2 × $^3J_{PH}$| = 7.1 Hz, 18H, P-C(CH$_3$)$_3$), 1.19 (apparent t, |2 × $^3J_{PH}$| = 7.2 Hz, 18H, P-C(CH$_3$)$_3$), −41.99 (t, $^2J_{PH}$ = 13.0 Hz, 1H, Ir*H*). ^{31}P{^{1}H} NMR (C_6D_6, 202.46 MHz, 300 K): δ 106.0 (s). ^{13}C{^{1}H} NMR (C_6D_6, 125.76 MHz, 300 K): δ 158.4 (apparent t, |2 × $^2J_{PC}$| = 10.1 Hz, C_{Ar}), 125.1 (s, C_{Ar}), 101.5 (t, $^4J_{PC}$ = 5.7 Hz, C_{Ar}), 41.5 (apparent t, |2 × $^1J_{PC}$| = 12.2 Hz, C_q), 38.1 (apparent t, |2 × $^1J_{PC}$| = 13.0 Hz, C_q), 28.4 (apparent t, |2 × $^2J_{PC}$| = 2.7 Hz, CH$_3$), 28.3 (apparent t, |2 × $^2J_{PC}$| = 2.7 Hz, CH$_3$).

*^{tBu4}PNCOPIrHCl (**2f**).* From **1f** (428 mg, estimated purity 50%, ∼0.54 mmol) and [IrCl(COE)$_2$]$_2$ **2f** was obtained as a dark red solid (145 mg, 55% yield).

Anal. Calcd for $C_{22}H_{41}ClIrNOP_2$: C, 42.27; H, 6.61; N, 2.24. Found: C, 42.19; H, 6.57; N, 2.33. HRMS: calcd for $C_{22}H_{42}ClIrNOP_2$ [M + H$^+$], 626.2046; found, *m*/*z* 626.2057. ^{1}H NMR (C_6D_6, 500.13 MHz, 300 K): δ 6.86 (apparent t, |2 × $^3J_{HH}$| = 7.8 Hz, 1H, Ar-*H*), 6.72 (d, $^3J_{HH}$ = 7.9 Hz, 1H, Ar-*H*), 6.25 (d, $^3J_{HH}$ = 7.6 Hz, 1H, Ar-*H*), 4.12 (d, $^4J_{PH}$ = 3.1 Hz, 1H, N*H*), 1.35 (d, $^3J_{PH}$ = 14.2 Hz, 9H, P-C(C*H*$_3$)$_3$), 1.29 (d, $^3J_{PH}$ = 14.5 Hz, 9H, P-C(CH$_3$)$_3$), 1.19 (d, $^3J_{PH}$ = 13.9 Hz, 9H,

DOI: 10.1021/acs.organomet.7b00713
Organometallics XXXX, XXX, XXX−XXX

P-C(CH_3)$_3$), 1.15 (d, $^3J_{PH}$ = 14.1 Hz, 9H, P-C(CH_3)$_3$), −41.34 (apparent t, |2 × $^2J_{PH}$| = 13.1 Hz, 1H, Ir*H*). ^{31}P{^{1}H} NMR (C_6D_6, 202.46 MHz, 300 K): δ 171.5 (d, $^2J_{PP}$ = 357 Hz), 108.5 (d, $^2J_{PP}$ = 357 Hz). ^{13}C{^{1}H} NMR (CD_2Cl_2, 125.76 MHz, 300 K): δ 168.4 (apparent t, |$^2J_{PC}$ + $^3J_{PC}$| = 5.9 Hz, C_{Ar}), 158.5 (dd, $^3J_{PC}$ = 14.3 Hz, $^2J_{PC}$ = 5.4 Hz, C_{Ar}), 125.49 (s, C_{Ar}), 103.3 (d, $^3J_{PC}$ = 11.7 Hz, C_{Ar}), 102.5 (d, $^3J_{PC}$ = 11.5 Hz, C_{Ar}), 43.3 (dd, $^1J_{PC}$ = 19.3 Hz, $^3J_{PC}$ = 5.0 Hz, C_q), 42.0 (dd, $^1J_{PC}$ = 19.6 Hz, $^3J_{PC}$ = 3.8 Hz, C_q), 39.6 (dd, $^1J_{PC}$ = 21.5 Hz, $^3J_{PC}$ = 5.5 Hz, C_q), 38.7 (dd, $^1J_{PC}$ = 21.8 Hz, $^3J_{PC}$ = 3.6 Hz, C_q), 28.4 (apparent t, |2 × $^2J_{PC}$| = 4.6 Hz, CH_3), 27.9 (d, $^2J_{PC}$ = 4.8 Hz, CH_3), 27.7 (d, $^2J_{PC}$ = 4.9 Hz, CH_3)

*^{iPr2}PNCOP^{tBu2}IrHCl (**2g**).* From **1g** (1.7 mL, 0.3074 mM in toluene, 0.52 mmol) and [IrCl(COE)$_2$]$_2$ **2g** was obtained as a bright red solid (193 mg, 65% yield).

Anal. Calcd for $C_{20}H_{37}ClIrNOP_2$: C, 40.23; H, 6.25; N, 2.35. Found: C, 40.38; H, 6.14; N, 2.38. HRMS: calcd for $C_{20}H_{38}ClIrNOP_2$ [M + H$^+$], 598.1733; found, *m*/*z* 598.1740. ^{1}H NMR (C_6D_6, 499.93 MHz, 300 K): δ 6.87 (apparent t, |2 × $^3J_{HH}$| = 7.9 Hz, 1H, Ar-*H*), 6.73 (d, $^3J_{HH}$ = 7.9 Hz, 1H, Ar-*H*), 6.22 (d, $^3J_{HH}$ = 7.7 Hz, 1H, Ar-*H*), 3.69 (d, $^2J_{PH}$ = 3.4 Hz, 1H, N*H*), 2.48 (m, 1H, P-C*H*(CH_3)$_2$), 1.95 (m, 1H, P-C*H*(CH_3)$_2$), 1.33 (d, $^3J_{PH}$ = 14.0 Hz, 9H, P-C(CH_3)$_3$), 1.29 (d, $^3J_{PH}$ = 14.5 Hz, 9H, P-C(CH_3)$_3$), 1.23−1.12 (m, 6H, P-CH(CH_3)$_2$), 0.87−0.80 (m, 6H, P-CH(CH_3)$_2$), −39.79 (apparent t, |2 × $^2J_{PH}$| = 13.2 Hz, 1H, Ir*H*). ^{31}P{^{1}H} NMR (C_6D_6, 202.46 MHz, 300 K): δ 175.1 (d, $^2J_{PP}$ = 362 Hz), 103.1 (d, $^3J_{PP}$ = 362 Hz). ^{13}C{^{1}H} NMR (C_6D_6, 125.76 MHz, 300 K): δ 168.0 (apparent t, |$^2J_{PC}$ + $^3J_{PC}$| = 5.4 Hz, C_{Ar}), 157.3 (dd, $^2J_{PC}$ = 15.1 Hz, $^3J_{PC}$ = 4.6 Hz, C_{Ar}), 125.4 (s, C_{Ar}), 113.9 (s, C_{Ar}), 103.9 (d, $^3J_{PC}$ = 12.2 Hz, C_{Ar}), 103.2 (d, $^3J_{PC}$ = 11.8 Hz, C_{Ar}), 43.9 (dd, $^1J_{PC}$ = 18.5 Hz, $^3J_{PC}$ = 5.4 Hz, C_q), 39.3 (dd, $^1J_{PC}$ = 20.3 Hz, $^3J_{PC}$ = 5.4 Hz, C_q), 28.8 (d, $^2J_{PC}$ = 3.3 Hz, CH_3), 28.5 (d, $^2J_{PC}$ = 3.0 Hz, CH_3), 27.9 (d, $^2J_{PC}$ = 5.3 Hz, CH_3), 27.7 (d, $^2J_{PC}$ = 5.5 Hz, CH_3), 27.4 (d, $^2J_{PC}$ = 2.6 Hz, CH_3), 17.8 (s, CH), 17.6 (m, CH), 16.8 (s, CH).

*^{Cy2}PNCOP^{tBu2}IrHCl (**2h**).* From **1h** (242 mg, 0.5 mmol) and [IrCl(COE)$_2$] (197 mg, 0.22 mmol) **2h** was obtained as a bright red-pink solid (161 mg, 54% yield).

Anal. Calcd for $C_{26}H_{45}ClIrNOP_2$: C, 46.11; H, 6.70; N, 2.07. Found: C, 46.27; H, 6.86; N, 2.08. HRMS: calcd for $C_{26}H_{46}ClIrNOP_2$ [M + H$^+$], 678.2359; found, *m*/*z* 678.2362. ^{1}H NMR (C_6D_6, 500.13 MHz, 300 K): δ 6.91 (apparent t, |2 × $^3J_{HH}$| = 7.8 Hz, 1H, Ar-*H*), 6.75 (d, $^3J_{HH}$ = 7.8 Hz, 1H, Ar-*H*), 6.34 (d, $^3J_{HH}$ = 7.8 Hz, 1H, Ar-*H*), 3.93 (d, $^2J_{PH}$ = 2.7 Hz, 1H, N*H*), 2.50−2.40 (m, 2H, Cy*H*), 2.,03−1.42 (m, 12 H, Cy*H*), 1.35 (d, $^3J_{PH}$ = 14.2 Hz, 9H, P-C(CH_3)$_3$), 1.30 (d, $^3J_{PH}$ = 14.4 Hz, 9H, P-C(CH_3)$_3$), 1.27−0.93 (m, 8H, Cy*H*), −39.89 (apparent t, |2 × $^2J_{PH}$| = 13.1 Hz, 1H, Ir*H*). ^{31}P{^{1}H} NMR (C_6D_6, 202.46 MHz, 300 K): δ 175.2 (d, $^2J_{PP}$ = 361 Hz), 95.9 (d, $^2J_{PP}$ = 361 Hz). ^{13}C{^{1}H} NMR (C_6D_6, 125.76 MHz, 300 K): δ 168.0 (apparent t, |$^2J_{PC}$ + $^3J_{PC}$| = 5.6 Hz, C_{Ar}), 157.6 (dd, $^2J_{PC}$ = 15.3 Hz, $^3J_{PC}$ = 5.7 Hz, C_{Ar}), 125.4 (s, C_{Ar}), 114.2 (s, C_{Ar}), 103.9 (d, $^3J_{PC}$ = 12.2 Hz, C_{Ar}), 103.0 (d, $^3J_{PC}$ = 10.9 Hz, C_{Ar}), 43.8 (dd, $^1J_{PC}$ = 18.7 Hz, $^3J_{PC}$ = 5.3 Hz, C_q), 39.3 (dd, $^1J_{PC}$ = 20.3 Hz, $^3J_{PC}$ = 5.6 Hz, C_q), 38.8 (dd, $^1J_{PC}$ = 29.3 Hz, $^3J_{PC}$ = 2.7 Hz, CH), 36.7 (dd, $^1J_{PC}$ = 30.9 Hz, $^3J_{PC}$ = 2.1 Hz, CH), 28.0 (s, CH_2), 27.9 (d, $^2J_{PC}$ = 5.6 Hz, CH_3), 27.7 (d, $^2J_{PC}$ = 5.1 Hz, CH_3), 27.4 (d, $^2J_{PC}$ = 3.4 Hz, CH_2), 27.1 (s, CH_2), 27.0 (d, $^3J_{PC}$ = 4.1 Hz, CH_2) 26.9 (d, $^4J_{PC}$ = 4.8 Hz, CH_2), 26.8 (d, $^4J_{PC}$ = 3.9 Hz, CH_2), 26.2 (s, CH_2), 26.1 (s, CH_2).

*^{tBu4}PNCNPIr(CO) (**3e**).* In a glovebox, **2e** (24 mg, 40 μmol) and sodium *tert*-butoxide (7 mg, 72 μmol) were weighed in to a Schlenk flask inside a glovebox. C_6D_6 (2 mL) and COE (0.1 mL, 770 μmol) were added, and the reaction mixture was heated to 90 °C for 1 h and then cooled to room temperature. CO was then bubbled through the solution, whereupon the color changed from dark orange to yellow; the CO flow was maintained for 10 min to ensure completion of the reaction. The solution was transferred into a separate Schlenk flask by filtration, and the volatiles were removed in vacuo; the resulting orange residue was washed with the minimum amount of pentane to afford a yellow solid. ^{31}P NMR analysis revealed quantitative conversion to the carbonyl complex **3e**.

HRMS: calcd for $C_{23}H_{42}ClIrN_2OP_2$ [M + H$^+$], 617.2397; found, *m*/*z* 617.2419. IR (DCM, cm^{-1}): ν_{CO} 1919.5. ^{1}H NMR (CD_2Cl_2, 499.93 MHz, 300 K): δ 6.62 (t, $^3J_{HH}$ = 7.7 Hz, 1H, Ar-*H*), 6.19 (d, $^3J_{HH}$ = 7.7 Hz, 2H, Ar-*H*), 4.68 (br s, 2H, N*H*), 1.36 (apparent t, |$^3J_{PH}$| = 7.1 Hz, P-C(CH_3)$_3$). ^{31}P{^{1}H} NMR (CD_2Cl_2, 202.46 MHz, 300 K): δ 129.4 (s). ^{13}C{^{1}H} NMR (CD_2Cl_2, 125.76 MHz, 300 K): δ 199.7 (t, $^2J_{PC}$ = 6.2 Hz, Ir-CO), 161.4 (apparent t, |$^2J_{PC}$ + $^3J_{PC}$| = 12.7 Hz, C_{Ar}), 128.2 (s, C_{Ar}), 99.9 (apparent t, |$^3J_{PC}$ + $^4J_{PC}$| = 6.5 Hz, C_{Ar}), 39.7 (apparent t, |$^1J_{PC}$ + $^3J_{PC}$| = 13.2 Hz, C_q), 29.0 (apparent t, |$^2J_{PC}$ + $^3J_{PC}$| = 3.0 Hz, CH_3).

*^{tBu4}PNCOPIr(CO) (**3f**).* In a glovebox, ^{tBu}PNCOP^{tBu}IrHCl (**2f**; 26 mg, 42 μmol) and sodium *tert*-butoxide (7 mg, 72 μmol) were weighed into a Schlenk flask inside a glovebox. C_6D_6 (4 mL) was then added under argon. The solution was stirred vigorously under hydrogen for 2 h, during which time the solution turned from dark red to orange. Despite the addition of further sodium *tert*-butoxide (3.5 mg, 36 mmol), the reaction did not go to completion and the conversion of **2f** was 90%, as indicated by ^{31}P{^{1}H} NMR. The hydrogen in the Schlenk flask was replaced with CO, and the solution was stirred vigorously under CO, whereupon it rapidly turned yellow; the reaction mixture was stirred under CO for a further 20 min. The solution was transferred via cannula filtration into a separate Schlenk flask, and the solvent was removed in vacuo to afford **3f** as a yellow solid showing over 90% purity by ^{31}P NMR.

HRMS: calcd for $C_{23}H_{41}ClIrNO_2P_2$ [M + H$^+$], 618.2237; found, *m*/*z* 618.2266. IR (DCM, cm^{-1}): ν_{CO} 1928.2. ^{1}H NMR (C_6D_6, 500.13 MHz, 300 K): δ 6.96 (apparent t, |2 × $^3J_{HH}$|= 7.8 Hz, 1H, Ar-*H*), 6.82 (d, $^3J_{HH}$ = 8.0 Hz, 1H, Ar-*H*), 6.39 (d, $^3J_{HH}$ = 7.6 Hz, 1H, Ar-*H*), 4.38 (d, $^2J_{PH}$ = 2.7 Hz, 1H, N*H*), 1.36 (d, $^3J_{PH}$ = 14.3 Hz, 18H, P-C(CH_3)$_3$), 1.21 (d, $^3J_{PH}$ = 13.9 Hz, 18H, P-C(CH_3)$_3$). ^{31}P{^{1}H} NMR (C_6D_6, 202.46 MHz, 300 K): δ 195.5 (d, $^2J_{PP}$ = 301 Hz), 128.9 (d, $^2J_{PH}$ = 302 Hz). ^{13}C{^{1}H} NMR (C_6D_6, 125.76 MHz, 300 K): δ 199.8 (apparent t, |2 × $^2J_{PC}$| = 5.5 Hz, Ir-CO), 129.0 (s, C_{Ar}), 102.6 (d, $^3J_{PC}$ = 13.2 Hz, C_{Ar}), 101.9 (d, $^3J_{PC}$ = 13.0 Hz, C_{Ar}), 41.0 (dd, $^1J_{PC}$ = 22.7 Hz, $^3J_{PC}$ = 3.1 Hz, C_q), 39.4 (d, $^1J_{PC}$ = 23.6 Hz, C_q), 28.9 (d, $^2J_{PC}$ = 6.0 Hz, CH_3), 28.6 (d, $^2J_{PC}$ = 6.2 Hz, CH_3).

Crystallography. X-ray diffraction data for iridium hydrido chloro complexes were collected at either 173 K (**2e**,**f**) or 93 K (**2h**) by using a Rigaku FR-X Ultrahigh Brilliance Microfocus RA generator/confocal optics and XtaLAB P200 system, with Mo Kα radiation (λ = 0.71075 Å). Diffraction data for compound **2g** were collected at 173 K by using a Rigaku MM-007HF High Brilliance RA generator/confocal optics and XtaLAB P100 system, with Cu Kα radiation (λ = 1.54187 Å). Intensity data were collected using either just ω steps or both ω and φ steps, accumulating area detector images spanning at least a hemisphere of reciprocal space. All data were corrected for Lorentz−polarization effects. A multiscan absorption correction was applied by using either CrystalClear[37] or CrysAlisPro.[38] Structures were solved by Patterson (DIRDIF99 PATTY[39]) or dual-space (SHELXT[40]) methods and refined by full-matrix least squares against F^2 (SHELXL-2016[41]). Non-hydrogen atoms were refined anisotropically, and hydrogen atoms bound to carbon were refined using a riding model. Hydrogen atoms bound to nitrogen or iridium were located from the difference Fourier map and refined isotropically subject to a distance restraint. All calculations were performed using the CrystalStructure[42] interface. Crystallographic data for the four complexes have been deposited with the Cambridge Crystallographic Data Centre as CCDC 1570250−1570253.

General Procedure for the Transfer Dehydrogenation of COA with TBE. Catalyst testing was conducted in a Fischer−Porter bottle with a volume of ∼20 mL. The predried Fischer−Porter bottle was charged with the required amount of sodium *tert*-butoxide and then evacuated and back-filled with argon three times in a Schlenk line. COA (1.2 mL) and TBE (1.15 mL) were added by syringe under argon flow followed by a solution of the precatalyst (0.3 mL, 10 mM in toluene, 3 μmol). The Fischer−Porter bottle was heated in a sand bath of ∼1 cm above the liquid level. The apparatus was heated to 200 °C for 6 h with a stirring rate of 400 rpm under an autogenous pressure of ∼2 bar. At the end of the reaction, the bottle was cooled with an ice−water bath and the liquid product was analyzed by an Agilent 6850N GC instrument equipped with a GS-GASPRO column (60 m × 0.32 mm × 0.5 μm). Oven temperature program: isothermal at 220 °C for 30 min, then 5 °C/min to 250 °C and hold at 250 °C for 30 min. The

DOI: 10.1021/acs.organomet.7b00713
Organometallics XXXX, XXX, XXX−XXX

concentrations of hydrocarbon reactants and products were determined using external standards.

■ ASSOCIATED CONTENT

Supporting Information

The Supporting Information is available free of charge on the ACS Publications website at DOI: 10.1021/acs.organomet.7b00713.

Synthesis and characterization of iridium hydrido chloro carbonyl pincer complexes, ESI-MS of iridium pincer complexes, crystallographic parameters for **2e**,**f**,**h**, NMR data for all compounds, preparation of **3e** from **2e** via iridium hydride intermediate, and attempted preparation of **3g**,**h** (PDF)

Accession Codes

CCDC 1570250−1570253 contain the supplementary crystallographic data for this paper. These data can be obtained free of charge via www.ccdc.cam.ac.uk/data_request/cif, or by emailing data_request@ccdc.cam.ac.uk, or by contacting The Cambridge Crystallographic Data Centre, 12 Union Road, Cambridge CB2 1EZ, UK; fax: +44 1223 336033.

■ AUTHOR INFORMATION

Corresponding Author

*E-mail for J.L.: liujianke@hotmail.com.

ORCID

David B. Cordes: 0000-0002-5366-9168

Jianke Liu: 0000-0002-4190-9195

Notes

The authors declare no competing financial interest.

■ ACKNOWLEDGMENTS

We thank Dr. Sven Tobisch, Dr. Philip Dyer and Prof. David Cole-Hamilton for helpful discussions. We also thank Sasol for permission to publish this work.

■ REFERENCES

(1) Jensen, C. *Chem. Commun.* **1999**, *24*, 2443−2449.

(2) Kumar, A.; Goldman, A. S. In *The Privileged Pincer-Metal Platform: Coordination Chemistry & Applications*; van Koten, G., Gossage, R. A., Eds.; Springer International Publishing: Cham, Switzerland, 2016; pp 307−334.

(3) Gao, Y.; Guan, C.; Zhou, M.; Kumar, A.; Emge, T. J.; Wright, A. M.; Goldberg, K. I.; Krogh-Jespersen, K.; Goldman, A. S. *J. Am. Chem. Soc.* **2017**, *139*, 6338−6350.

(4) Roddick, D. M. In *Organometallic Pincer Chemistry*; van Koten, G., Milstein, D., Eds.; Springer Berlin Heidelberg: Berlin, Heidelberg, 2013; Vol. *40*, pp 49−88.

(5) Shih, W.-C.; Ozerov, O. V. *Organometallics* **2017**, *36*, 228−233.

(6) Polukeev, A. V.; Wendt, O. F. *Organometallics* **2017**, *36*, 639−649.

(7) Stoutland, P. O.; Bergman, R. G.; Nolan, S. P.; Hoff, C. D. *Polyhedron* **1988**, *7* (16), 1429−1440.

(8) Gupta, M.; Hagen, C.; Flesher, R. J.; Kaska, W. C.; Jensen, C. M. *Chem. Commun.* **1996**, *17*, 2083−2084.

(9) Kundu, S.; Choliy, Y.; Zhuo, G.; Ahuja, R.; Emge, T. J.; Warmuth, R.; Brookhart, M.; Krogh-Jespersen, K.; Goldman, A. S. *Organometallics* **2009**, *28*, 5432−5444.

(10) Punji, B.; Emge, T. J.; Goldman, A. S. *Organometallics* **2010**, *29*, 2702−2709.

(11) Goettker-Schnetmann, I.; White, P.; Brookhart, M. *J. Am. Chem. Soc.* **2004**, *126*, 1804−1811.

(12) Nawara-Hultzsch, A. J.; Hackenberg, J. D.; Punji, B.; Supplee, C.; Emge, T. J.; Bailey, B. C.; Schrock, R. R.; Brookhart, M.; Goldman, A. S. *ACS Catal.* **2013**, *3*, 2505−2514.

(13) Yao, W.; Zhang, Y.; Jia, X.; Huang, Z. *Angew. Chem., Int. Ed.* **2014**, *53*, 1390−1394.

(14) Yao, W.; Jia, X.; Leng, X.; Goldman, A. S.; Brookhart, M.; Huang, Z. *Polyhedron* **2016**, *116*, 12−19.

(15) Goldman, A. S.; Renkema, K. B.; Czerw, M.; Krogh-Jespersen, K. *ACS Symp. Ser.* **2004**, *885*, 198−215.

(16) Kumar, A.; Bhatti, T. M.; Goldman, A. S. *Chem. Rev.* **2017**, *117* (19), 12357−12384.

(17) Choi, J.; MacArthur, A. H. R.; Brookhart, M.; Goldman, A. S. *Chem. Rev.* **2011**, *111* (3), 1761−1779.

(18) Zhang, Y.; Yao, W.; Fang, H.; Hu, A.; Huang, Z. *Sci. Bull.* **2015**, *60* (15), 1316−1331.

(19) Benito-Garagorri, D.; Bocokić, V.; Mereiter, K.; Kirchner, K. *Organometallics* **2006**, *25* (16), 3817−3823.

(20) Murugesan, S.; Stoeger, B.; Weil, M.; Veiros, L. F.; Kirchner, K. *Organometallics* **2015**, *34*, 1364−1372.

(21) Baroudi, A.; El-Hellani, A.; Bengali, A. A.; Goldman, A. S.; Hasanayn, F. *Inorg. Chem.* **2014**, *53*, 12348−12359.

(22) Bordwell, F. G.; Branca, J. C.; Hughes, D. L.; Olmstead, W. N. *J. Org. Chem.* **1980**, *45* (16), 3305−3313.

(23) Gawron, O.; Duggan, M.; Grelecki, C. J. *Anal. Chem.* **1952**, *24* (6), 969−970.

(24) Ozerov, O. V.; Guo, C.; Foxman, B. M. *J. Organomet. Chem.* **2006**, *691* (22), 4802−4806.

(25) Hrobárik, P.; Hrobáriková, V.; Meier, F.; Repiský, M.; Komorovský, S.; Kaupp, M. *J. Phys. Chem. A* **2011**, *115* (22), 5654−5659.

(26) Bistoni, G.; Rampino, S.; Scafuri, N.; Ciancaleoni, G.; Zuccaccia, D.; Belpassi, L.; Tarantelli, F. *Chem. Sci.* **2016**, *7* (2), 1174−1184.

(27) Goettker-Schnetmann, I.; White, P. S.; Brookhart, M. *Organometallics* **2004**, *23*, 1766−1776.

(28) Huang, Z.; Brookhart, M.; Goldman, A. S.; Kundu, S.; Ray, A.; Scott, S. L.; Vicente, B. C. *Adv. Synth. Catal.* **2009**, *351*, 188−206.

(29) Goldberg, J. M.; Cherry, S. D. T.; Guard, L. M.; Kaminsky, W.; Goldberg, K. I.; Heinekey, D. M. *Organometallics* **2016**, *35*, 3546−3556.

(30) Goldberg, J. M.; Wong, G. W.; Brastow, K. E.; Kaminsky, W.; Goldberg, K. I.; Heinekey, D. M. *Organometallics* **2015**, *34*, 753−762.

(31) Macrae, C. F.; Bruno, I. J.; Chisholm, J. A.; Edgington, P. R.; McCabe, P.; Pidcock, E.; Rodriguez-Monge, L.; Taylor, R.; van de Streek, J.; Wood, P. A. *J. Appl. Crystallogr.* **2008**, *41* (2), 466−470.

(32) Rimoldi, M.; Mezzetti, A. *Inorg. Chem.* **2014**, *53*, 11974−11984.

(33) Cordero, B.; Gomez, V.; Platero-Prats, A. E.; Reves, M.; Echeverria, J.; Cremades, E.; Barragan, F.; Alvarez, S. *Dalton Trans.* **2008**, *21*, 2832−2838.

(34) Renkema, K. B.; Kissin, Y. V.; Goldman, A. S. *J. Am. Chem. Soc.* **2003**, *125*, 7770−7771.

(35) Morello, G. R.; Hopmann, K. H. *ACS Catal.* **2017**, *7*, 5847−5855.

(36) Tanaka, R.; Yamashita, M.; Nozaki, K. *J. Am. Chem. Soc.* **2009**, *131*, 14168−14169.

(37) *CrystalClear-SM Expert v2.1*; Rigaku Americas, The Woodlands, TX, USA, and Rigaku Corporation, Tokyo, Japan, 2015.

(38) *CrysAlisPro v1.171.38.43i and v. 1.171.39.8*; Rigaku Oxford Diffraction, Rigaku Corporation, Oxford, U.K., 2015.

(39) Beurskens, P. T.; Beurskens, G.; de Gelder, R.; Garcia-Granda, S.; Gould, R. O.; Israel, R.; Smits, J. M. M. *DIRDIF-99*; Crystallography Laboratory, University of Nijmegen, Nijmegen, The Netherlands, 1999.

(40) Sheldrick, G. *Acta Crystallogr., Sect. A: Found. Adv.* **2015**, *71* (1), 3−8.

(41) Sheldrick, G. *Acta Crystallogr., Sect. C: Struct. Chem.* **2015**, *71* (1), 3−8.

(42) *CrystalStructure v4.2*; Rigaku Americas, The Woodlands, TX, USA, and Rigaku Corporation, Tokyo, Japan, 2015.

DOI: 10.1021/acs.organomet.7b00713
Organometallics XXXX, XXX, XXX−XXX